ELSEVIER

Polymer 43 (2002) 289–300

polymer

www.elsevier.com/locate/polymer

# Fracture behaviour of polyethylene naphthalate (PEN)

A. Arkhireyeva, S. Hashemi*

*School of Polymer Technology, University of North London, Holloway Road, London N7 8DB, UK*

Received 5 June 2001; received in revised form 20 August 2001; accepted 12 September 2001

**Abstract**

Fracture toughness of a semi-crystalline polyethylene naphthalate (PEN) film of thicknesses 0.050, 0.075 and 0.125 mm was measured as a function of temperature and loading rate using both double edge notched tension (DENT) and single edge notched tension (SENT) specimens. The specific essential work of fracture (EWF) and the multi-specimen *J*-integral methods were used to evaluate fracture toughness. The variation of the specific total work of fracture ($w_f$) with ligament length ($L$) was linear for ligament lengths between 5 and 15 mm. Within this range, $w_f$ versus $L$ was independent of thickness at all temperatures but was dependent on both temperature and loading rate. The specific EWF ($w_e$) was found to be independent of thickness and loading rate but showed three regions of varying temperature dependence. Between 23 and 80°C (region I) $w_e$ was essentially independent of temperature but increased with temperature between 80 and 120°C (region II) and decreased with temperature thereafter (region III). At glass transition temperature (i.e. 120°C), $w_e$ reached a maximum value of 75 kJ/m$^2$. The specific non-EWF ($\beta w_p$) increased with both loading rate and temperature. The greatest change in $\beta w_p$ value with respect to temperature was obtained in region II.

The plot of *J*-integral versus crack extension ($\Delta a$) was independent of thickness but was dependent upon temperature. $w_e$ was found to be equivalent to both $J_{0.2}$ and $J_0$. 

*Keywords*: *J*-Integral; Fracture; Polyethylene naphthalate

## 1. Introduction

It is well established that when failure of notched specimens is brittle in nature, the area in which energy is dissipated near the crack tip is so small that the entire specimen can be assumed to exhibit Hookean elasticity. This type of failure can be studied using linear elastic fracture mechanics (LEFM).

As the extent of plastic deformation at the crack tip increases, the energy dissipation is no longer confined to a small region near the crack tip. Consequently, deviations from LEFM could become so significant that this type of analysis is no longer an adequate representation of the system. Although the *J-integral* has been traditionally used to quantify fracture toughness under large-scale crack tip plasticity, recently, EWF has been employed extensively as an alternative method, e.g. Refs. [1–22].

The work presented in this paper investigates the effect of specimen thickness, specimen geometry, temperature and the loading rate on the EWF of a semi-crystalline PEN film. The equivalence between EWF and *J*-integral is also examined using the multi-specimen *R*-curve method for determining the *J*-integral parameters.

## 2. Fracture mechanics concepts

### 2.1. Essential work of fracture

The EWF concept was first developed by Broberg [23] who suggested that the non-elastic region around the crack tip can be divided into two regions as depicted in Fig. 1a, referred to as the *inner fracture process zone* (IFPZ) and the *outer plastic deformation zone* (OPDZ). The IFPZ is where the actual fracture takes place and the OPDZ is where various types of deformation such as shear yielding and microvoiding may be operating. Based on this concept, total work of fracture, $W_f$, of a cracked body is then partitioned into two components: (i) the EWF, $W_e$, which is the work performed in the IFPZ and (ii) the non-EWF, $W_p$, which is the work performed in the OPDZ. Thus

$$W_f = W_e + W_p \quad (1)$$

When both the IFPZ and the OPDZ are contained in the ligament, then $W_e$ is proportional to the ligament length, $L$ and the $W_p$ is proportional to the square of the ligament

* Corresponding author. Tel.: +44-0207-7535128; fax: +44-7535081.
*E-mail address:* s.hashemi@unl.ac.uk (S. Hashemi).

0032-3861/02/$ - see front matter 
PII: S0032-3861(01)00623-1

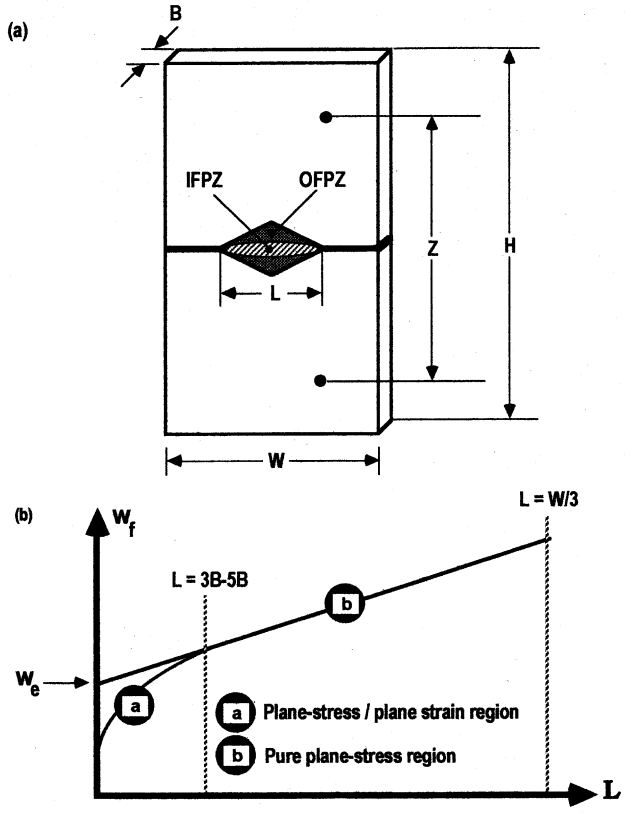


Fig. 1. Schematic representation of: (a) IFPZ and the OPDZ, (b) specific work of fracture ($w_f$) versus ligament length ($L$).

length, $L^2$. Hence it can be written

$$W_e = w_e BL, \qquad W_p = \beta w_p BL^2 \tag{2}$$

where $w_e$ is termed the specific EWF and $\beta w_p$ is termed the specific non-essential work of fracture. The parameter $\beta$ is proportionality constant (plastic zone shape factor) whose value depends on the geometry of the specimen and the crack. Introducing relationships in Eq. (2) into Eq. (1) gives

$$w_f = w_e + \beta w_p L \tag{3}$$

where $w_f$ is the specific total work of fracture.

According to Eq. (3), plotting $w_f$ against ligament length yield a straight line whose intercept with the $w_f$-axis gives $w_e$ and whose slope is $\beta w_p$ as shown in Fig. 1b.

The physical meaning of $w_e$ can be interpreted by taking a contour integral around the edge of a fully developed fracture process of length $\rho$ and width $d$ formed at the crack tip. $w_e$ may be considered as that work dissipated in the fracture process zone at the crack tip. This includes the plastic work up to necking in the material that is to form the process zone ($w_{eI}$) and the work to fracture the neck ($w_{eII}$).

If it is assumed that there is uniform straining up to necking then

$$w_{eI} = d\int_0^{\bar{e}_n} \bar{\sigma}\, \mathrm{d}\bar{e}$$

where $\bar{\sigma}$ and $\bar{e}$ are the true stress and strain, respectively, and $\bar{e}_n$ is the true strain at necking (note that $\int \bar{\sigma}\, \mathrm{d}\bar{e}$ is the local strain energy density). After necking, the deformation in the process zone is localised and non-uniform. If it is assumed that fracture occurs when the crack tip is further stretched so that crack opening displacement ($\delta$) is reached a critical value $\delta_c$ then

$$w_{eII} = \int_{de_n}^{\delta_c} \sigma(\delta)\, \mathrm{d}\delta$$

where $\sigma$ and $e_n$ are the engineering stress and strain at necking, respectively. The specific EWF ($w_e$) is the sum of the two integrals, i.e.

$$w_e = d\int_0^{\bar{e}_n} \bar{\sigma}\, \mathrm{d}\bar{e} + \int_{e_n d}^{\delta_c} \sigma(\delta)\, \mathrm{d}\delta \tag{4}$$

According to Eq. (4), since $d$ and $\delta_c$ are both expected to vary with thickness, $B$, hence $w_e$ should also vary with thickness. For this reason $w_e$ is regarded as a material constant for a given thickness.

### 2.1.1. Date qualifying scheme for EWF

In the heart of the EWF analysis are the following four key assumptions:

(i) Geometrical similarity exists between specimens of different ligament lengths during crack growth.
(ii) Ligament length is fully yielded prior to the onset of crack propagation.
(iii) Ligament length controls the size of the OPDZ and the volume of the zone is proportional to the square of the ligament length.
(iv) Fracture is under pure *plane-stress* conditions thus $w_e$ and $\beta w_p$ are both independent of the ligament length.

To satisfy these assumptions and hence to maintain the linearity between $w_f$ and $L$ as expressed by Eq. (3), it has been recommended that ligament length meet the following pre-requisites, e.g. Ref. [11]:

(i) $> L \leq 2R_p$. This ensures that complete yielding of the ligament region occurs prior to crack growth, hence maintaining the proportionality of $W_p$ and $L^2$. $R_p$ is the radius of the plastic zone at the crack tip.
(ii) $L \leq W/3$. This ensures that the size of the plastic zone is not disturbed by the lateral boundaries of the test specimen (edge effects) and therefore plastic deformation is confined to the ligament area.
(iii) $L \geq 3B - 5B$. This ensures that the state of stress in the ligament region is one of pure plane stress and not mixed mode in which case it will have both plane-stress and plane-strain characteristics and as a consequence of this both $w_e$ and $w_p$ become ligament length dependent.

The above restrictions on $L$, in effect, defines the valid ligament length range for plane-stress determination of the

EWF as [11]:

$$3B - 5B \le L \le \min\left(\frac{W}{3}, 2R_p\right) \tag{5}$$

The length $2R_p$ can be estimated from the following equation:

$$2R_p = \frac{1}{\pi}\frac{Ew_e}{\sigma_y^2} \tag{6}$$

where $E$ is Young's modulus and $\sigma_y$ is the uniaxial tensile yield stress of the material.

### 2.2. J-Integral

The equivalence between the critical value of the $J$-integral ($J_c$) and the specific EWF ($w_e$) has been investigated by several co-workers, e.g. Refs. [1–4,22].

The $J$-integral is a path-independent contour integral that describes the stresses, strains, and displacements of any path around a singular crack, if either linear or non-linear precedes crack growth. For a two-dimensional crack, the $J$-integral is given by

$$J = \int_\Gamma \left(W^* \, dy - T\frac{\partial U}{\partial x} ds\right) \tag{7}$$

where $(x,y)$ are rectangular coordinates normal to the crack front; $y$ is perpendicular to the surface of the crack; d$s$ is the increment of arc length along a contour $\Gamma$; $T$ and $u$ are stress and displacement vectors, respectively, acting on $\Gamma$; $W^*$ is the strain energy density.

Physically, the $J$-integral can be considered as the difference of the potential energy between two loaded identical specimens with slightly different crack lengths, i.e.

$$J = -\frac{1}{B}\frac{dU}{da} \tag{8}$$

where $U$ is the potential energy which can be obtained by measuring the area under the load–displacement curve, $a$ the crack length and $B$ is the thickness of the specimen.

Sumpter and Turner [24] proposed that $J$ can be separated into an elastic part $J_e$ and a plastic part $J_p$, so that

$$J = J_e + J_p \tag{9}$$

They subsequently defined $J$-integral as

$$J = \frac{1}{B(W-a)}(\eta_e U_e + \eta_p U_p) \tag{10}$$

where $U_e$ and $U_p$ are the elastic and plastic components of the total energy, respectively, as shown in Fig. 2a, and $\eta_e$ and $\eta_p$ are the corresponding work factors.

Previous study by the authors [22] has shown that certain combination of $a/W$ and the gauge length ($Z$) for single-edge notched tension (SENT) type specimens gives $\eta_e = \eta_p = \eta$, thus reducing Eq. (10) to

$$J = \frac{\eta U}{B(W-a)} \tag{11}$$

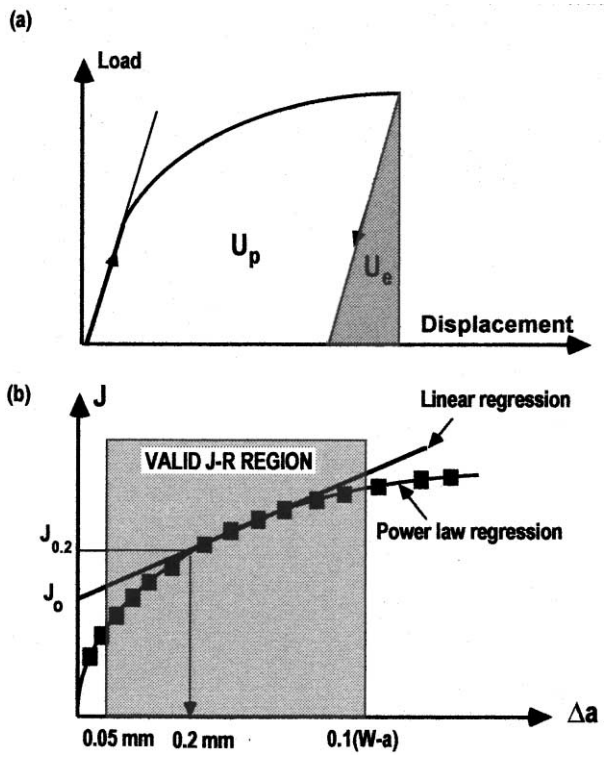


Fig. 2. Schematic representation of: (a) elastic and plastic partitioning of the total energy, (b) $J_R$-curve and ESIS data reduction scheme.

Eq. (11) provides the basic equation for the determination of the $J$-integral using a multiple specimen resistance curve ($J_R$-curve).

#### 2.2.1. Multi-specimen resistance curve ($J_R$-curve)

In this method, several identical specimens are monotonically loaded. Each specimen is loaded to a different displacement value and then unloaded to produce a different amount of crack extension ($\Delta a$) for a given value of $J$. The $J_R$-curve is then constructed by plotting the values of $J$ calculated using Eq. (11), against $\Delta a$.

At present two key standards [25,26] are available for determination of a valid $J_R$-curve for polymeric materials. These standards recommend two exclusion lines to be drawn parallel to the $J$-axis at 0.05 mm and 0.1$L$ offsets (or 10% of the original uncracked ligament length) as shown in Fig. 2b. The data points that fall between these two exclusion is then curve fitted by a simple power law equation of the form

$$J = C_1(\Delta a)^{C_2} \tag{12}$$

where the exponent parameter $C_2$ should be less than unity. The critical value of $J$ is then defined as the intersection of the $J_R$-curve with 0.2 mm offset line drawn parallel to the $J$-axis as depicted in Fig. 2b. In essence, $J_c$ is defined as $J_{0.2}$, at which point 0.2 mm crack growth has already occurred, i.e.

$$J_{0.2} = C_1(0.2)^{C_2} \tag{13}$$

The $J_{0.2}$ value is then considered a valid measurement if

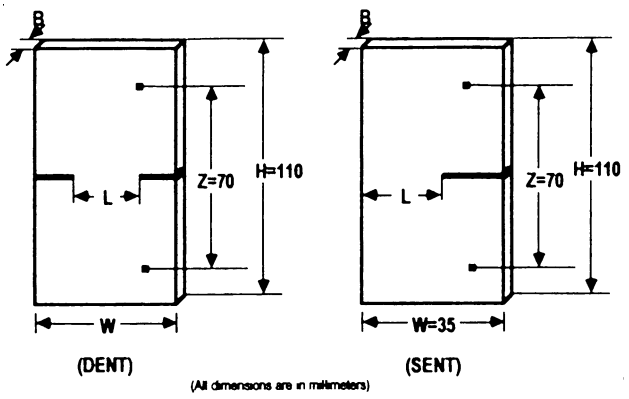


Fig. 3. DENT and SENT specimens.

the following $J$-controlled crack growth condition is satisfied [26]:

$$J_{0.2} \leq \min\left(\frac{W-a}{20}\sigma_y, \frac{B}{20}\sigma_y\right) \quad (14)$$

## 3. Experimental details

### 3.1. Material

This study was conducted on a semi-crystalline poly(-ethylene-naphthalate) having a degree of crystallinity of about 42% and a glass transition temperature of about 120–125°C, as measured by differential scanning calorimeter (DSC).

The material was received from Dupont UK (trade name 'Kaledex') in from of the A4 size sheets of nominal thicknesses 0.050, 0.075 and 0.125 mm.

### 3.2. EWF tests

EWF measurements were carried out on double-edge notched tension (DENT) and SENT specimens as shown in Fig. 3, having a constant width ($W$) of 35 mm and overall length ($H$) of 105 mm. These specimens were prepared by first cutting the sheets into rectangular coupons ($W = 35$ mm, $H = 105$ mm) and then notching each to a different ligament length value. After notching, specimens were tested to complete failure in an Instron testing machine using pneumatic clamps with an initial separation ($Z$) of 70 mm. The load–displacement ($P-\delta$) curve for each specimen was recorded using a computer data logger.

The effect of temperature on EWF parameters was investigated at displacement rate value of 5 mm/min between 23 and 140°C. The effect of loading rate was studied at 23°C between 2 and 50 mm/min, using only 0.075 mm thick DENT specimens.

### 3.3. J-Integral tests

Equivalence between EWF and $J$-integral was investigated at test temperatures of 23 and 80°C using the multiple-specimen $R$-curve method. SENT specimens with $W = 35$ mm and $Z = 70$ mm were loaded monotonically at a constant crosshead displacement rate of 5 mm/min.

To avoid partitioning $U$ into its elastic and plastic components, an $a/W$ ratio of 0.48 was selected. This ratio gives $\eta = 2.413$ [22]. The value of $J$-integral for each

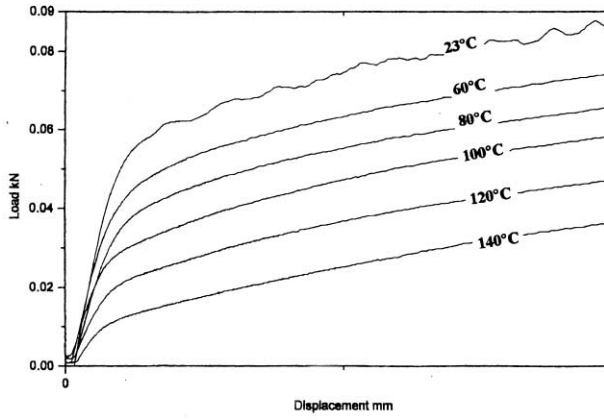


Fig. 4. Typical tensile load–displacement curves as a function of temperature.

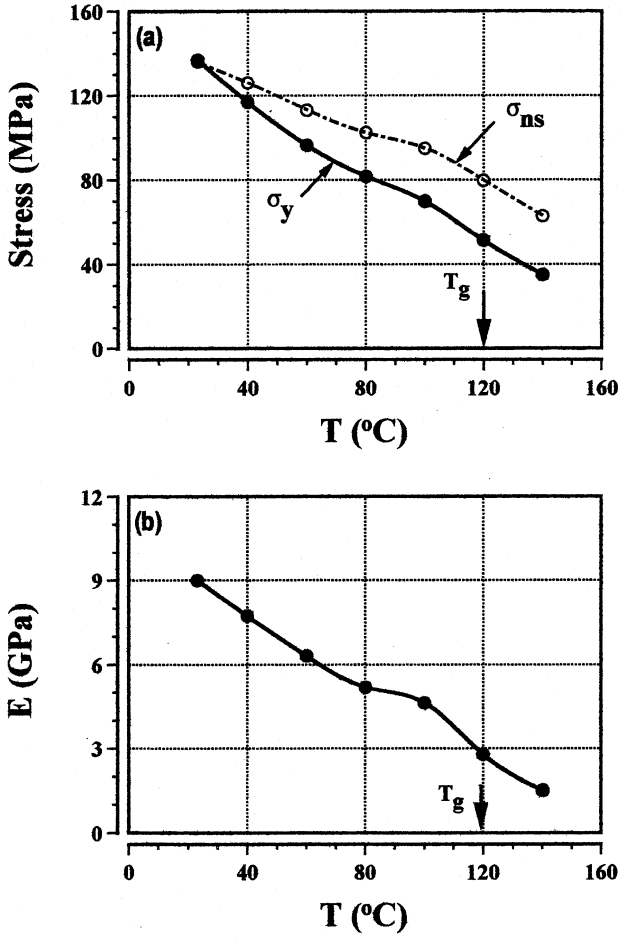


Fig. 5. (a) Tensile yield stress ($\sigma_y$) and maximum net-section stress ($\sigma_{ns}$) versus temperature, (b) tensile modulus ($E$) versus temperature.

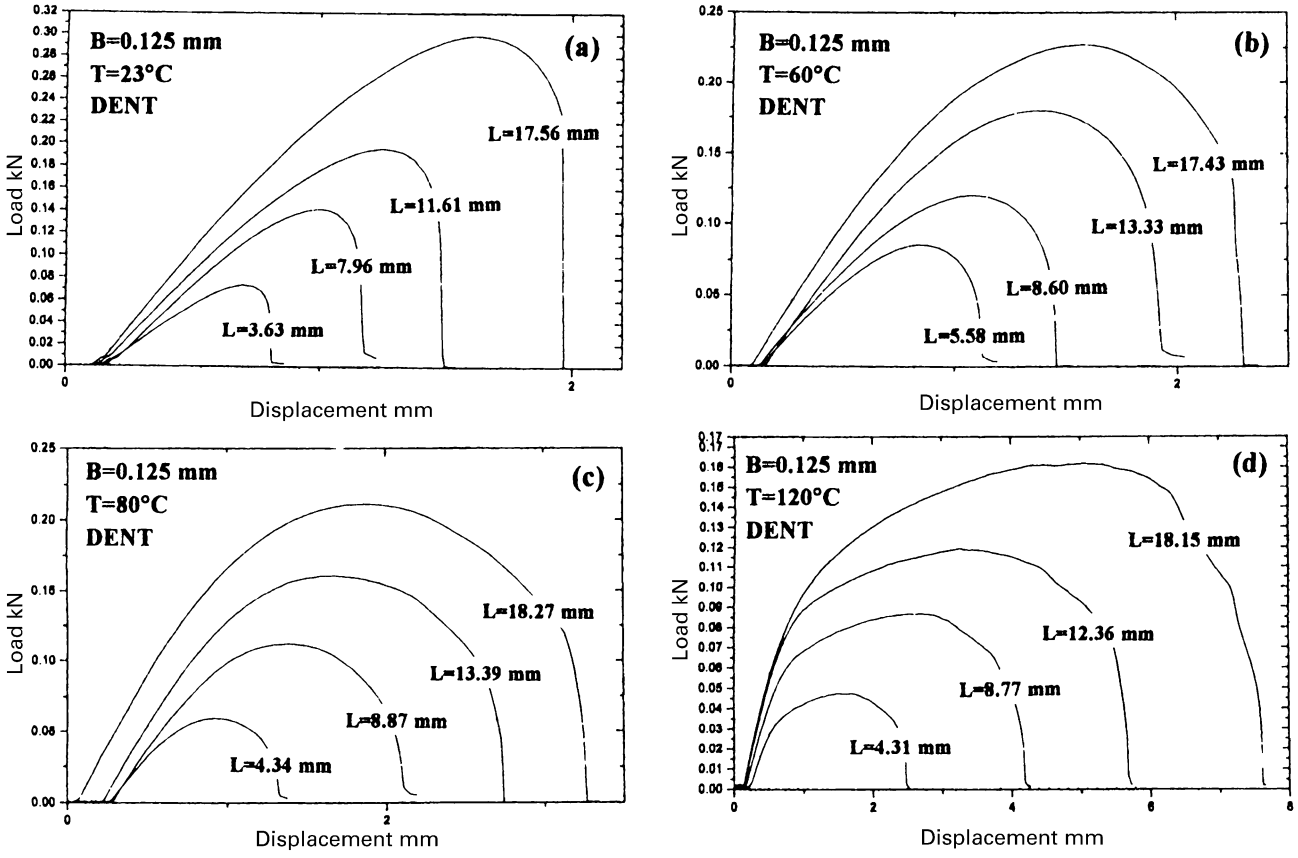


Fig. 6. Typical DENT type load–displacement curves.

specimen was calculated from the area under the load–displacement curve using Eq. (9). $J_R$-curve was then constructed and the $J_{0.2}$ value at each temperature was determined using the procedure described in Section 2.2.1.

### 3.4. Tensile tests

Measurements of the tensile yield stress and modulus were carried out between 23 and 140°C at a crosshead displacement rate value of 5 mm/min. These tests were performed on dumbbell-shaped specimens having a constant width of 3 mm in the gauge length region. Fig. 4 shows the influence of temperature on tensile load–displacement curves. It can be seen that tensile deformation of PEN specimens over the whole temperature range involves extensive yielding and strain hardening. As tensile load–displacement curves did not exhibit a clear load drop at yield point, the load at 1% strain was used for calculating the tensile yield stress. Tensile modulus was calculated using the initial slope of the curve.

Fig. 5 shows the effect of temperature on tensile yield stress and modulus. As expected, both properties decrease with increasing temperature due to viscoelasticity of the material.

## 4. Results and discussion

### 4.1. Fracture behaviour

The fracture of the DENT and SENT specimens occurred after ductile tearing of the ligament region producing load–displacement ($P-\delta$) curves examples of which are shown in Fig. 6 as a function of ligament length, thickness and temperature. It can be observed that variation in thickness and temperature had no major influence on the general behaviour of the $P-\delta$ curves. Although not shown, variation in loading rate had no major influence on the load–displacement ($P-\delta$) curves either.

The notable feature of the curves as a function of ligament length is their geometrical similarity, which is an essential pre-requisite for EWF testing. This observation as well as the contraction of specimen surfaces suggested that crack propagation in these specimens occurred under plane-stress conditions.

Although propagation of the crack in both DENT and SENT type specimens according to $P-\delta$ curves in Fig. 6 involved extensive crack tip yielding, it was not possible to detect visually if crack propagation occurred prior to full ligament yielding. The material in the plastic deformation zone had the same refractive index as the bulk material. For the same reason, it cannot be confirmed if ligament region

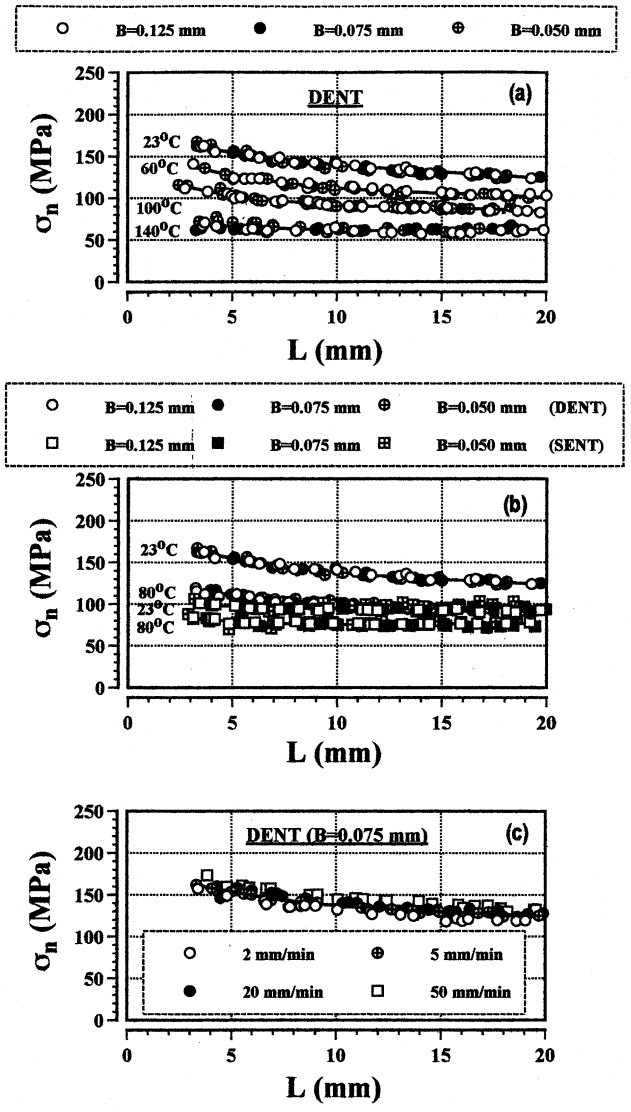


Fig. 7. Plots of net-section stress ($\sigma_n$) versus ligament length ($L$): (a) effect of specimen thickness for DENT type specimens at some selected temperatures, (b) effect of specimen geometry at two selected temperatures for all three thicknesses, (c) effect of loading rate for DENT type specimens of thickness 0.075 mm.

was fully yielded at maximum load. Nevertheless, attention was paid to the maximum load registered on the load–displacement curves.

Analysis by Hill [27] has shown that under plane-stress conditions, the maximum value of the net-section stress, $\sigma_n$ ($=$ maximum load divided by the ligament area) is independent of the ligament length, or as found experimentally, is only weakly dependent upon ligament length. The theoretical value under plane-stress conditions is given as $\sigma_n = 1.15\sigma_y$ for DENT type specimen and $\sigma_n = \sigma_y$ for SENT type specimen [27], where $\sigma_y$ is the tensile yield stress of the material. However, when ligament region has both plane-stress and plane-strain characteristics (i.e. mixed mode regime), which is often the case as ligament length falls below a threshold value, $\sigma_n$ then becomes dependent upon ligament length and its value increases with decreasing ligament length. Although experimentally, it is often difficult to locate precisely at what ligament length this stress state transition takes place (i.e. plane-stress to plane-stress/plane-strain), it is nevertheless possible to make a reasonable approximation of the threshold value.

Fig. 7 shows some typical examples highlighting the effect of specimen thickness, specimen geometry, temperature and loading rate, on the variation of net-section stress ($\sigma_n$) with ligament length ($L$). Plots demonstrate that the variation follows the general trend of decreasing $\sigma_n$ with increasing ligament length at small ligament lengths and tending towards a steady state value ($\sigma_{ns}$) at large ligament lengths. Evidently, $\sigma_n$ is not greatly influenced by the thickness of the specimen, but decreases with increasing temperature (see Fig. 5) and to a lesser extent, with decreasing rate. Further more as indicated by Fig. 7b, for the same temperature, the value of $\sigma_n$ for DENT specimens is consistently higher than for SENT specimens. Thus as preciously reported, e.g. Refs. [1,2,4,5,13,16,22], notch constraint effects in DENT type specimen is greater than in SENT type specimen.

As for the steady state value of net-section stress ($\sigma_{ns}$), it can be seen from Table 1 that the ratio $m = \sigma_{ns}/\sigma_y$ (known

Table 1
Effect of temperature on fracture parameters (Note: values in parenthesis refer to SENT type specimens)

| | Temperature (°C) | | | | | | |
|---|---|---|---|---|---|---|---|
| | 23 | 40 | 60 | 80 | 100 | 120 | 140 |
| $w_e$ (kJ/m$^2$) | 55.0 (60.54) | 54.54 (–) | 54.75 (–) | 54.74 (63.63) | 65.55 (–) | 75.72 (–) | 70.03 (–) |
| $\beta w_p$ (MJ/m$^3$) | 4.73 (4.08) | 5.15 (–) | 6.26 (–) | 9.54 (13.97) | 13.85 (–) | 21.38 (–) | 23.01 (–) |
| $2R_p$ (mm) | 8.4 | 9.8 | 11.82 | 13.52 | 19.72 | 25.45 | 27.21 |
| $m$ | 0.99 | 1.08 | 1.18 | 1.25 | 1.36 | 1.56 | 1.80 |
| $e_0$ (mm) | 0.64 | 0.65 | 0.72 | 0.78 | 0.88 | 1.25 | 1.43 |
| $J_{0.2}$ (kJ/m$^2$) | 55.25 | – | – | 61.45 | – | – | – |
| $dJ/da\|_{\Delta a=0.2}$ (MJ/m$^3$) | 112.88 | – | – | 170.35 | – | – | – |
| $(W-a)/20\sigma_y$ (kJ/m$^2$) | 124.62 | – | – | 74.42 | – | – | – |
| $B/20\sigma_y$ (kJ/m$^2$) | 0.342 | – | – | 0.204 | – | – | – |
| $J_0$ (kJ/m$^2$) | 54.39 | – | – | 55.66 | – | – | – |
| $dJ/da$ (MJ/m$^3$) | 51.63 | – | – | 95.23 | – | – | – |

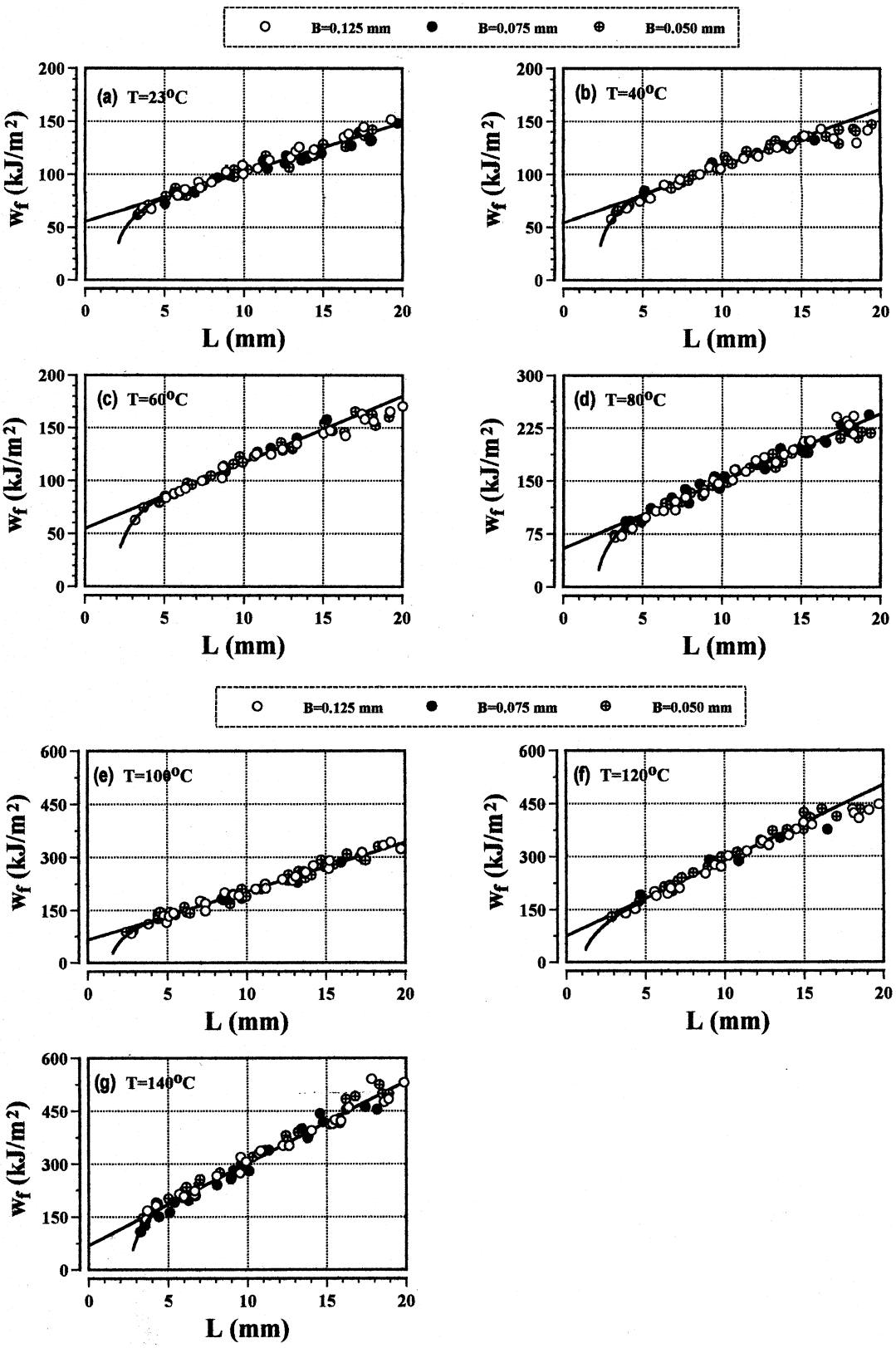


Fig. 8. Specific work of fracture ($w_f$) versus ligament length ($L$) for all three thicknesses between 23 and 140°C.

as the plastic constraint factor) increases with temperature, having values both smaller and greater than the theoretical value of 1.15. Indeed, previous studies, particularly on polymeric films, e.g. Refs. [6,9,10,13,17–19,21,22] have also indicated that Hill's prediction is not always achievable in practice. In fact, it is more or less accepted these days, that as long as $\sigma_n$ is not affected significantly by the length of the ligament region, EWF method should be applicable, whatever the value of $\sigma_{ns}$.

Another point in contention, is the ligament length at which stress state transition takes place. Although the proposed value of the lower ligament length threshold is three to five times the sample thickness, it has been frequently reported that for polymeric films [1,6,13,15–19,21,22] this threshold value is much greater than the proposed value. Plots in Fig. 7 further corroborate this, as it can be seen that stress-state transition in PEN occurs at a ligament length value of about 5–6 mm. This corresponds to $L/B$ ratio in the region of 40–100 at transition point, as thickness of the specimens is reduced from 0.125 to 0.05 mm. It is worth noting that the lower bound threshold value is not affected by the test variables. Contrary to what originally perceived, it is now believed that $L/B$ ratio at transition point does not have a universal value as it shows a strong dependence on the type of polymer being studied [1,6,13,15–19,21,22].

### 4.2. Essential and non-essential work of fracture parameters

#### 4.2.1. Effect of specimen thickness, B

Fig. 8 shows plots of the specific work of fracture, $w_f$, versus ligament length, $L$, for DENT type specimens for all three thicknesses between 23 and 140°C.

The notable feature of the plots over the entire temperature range is the insensitivity of $w_f$ values to thickness, which in turn suggests that $w_e$ and $\beta w_p$ values are insensitive to variation in thickness. The independence of $w_e$ on thickness implies that within the thickness range 0.125–0.050 mm, the width of the process zone and the crack opening displacement within the process zone are themselves insensitive to thickness variation (see Eq. (4)). The independence of $\beta w_p$ on thickness implies that either the shape of the plastic zone ($\beta$) and the work dissipated within the plastic deformation zone ($w_p$) are also invariant to thickness or that the change of one with thickness is offset by an equal and opposite change in the other.

Plots in Fig. 8 further indicate that for ligament lengths in the range 5–6 mm $\leq L \leq$ 15–16 mm, variation of $w_f$ with $L$ is essentially linear over the whole temperature range under consideration. Within this ligament length range, the size of the plastic zone thus increases in proportion to the ligament length. The departure from linearity for $L \leq$ 5–6 mm is attributed to the presence of a mixed mode stress state in the ligament region, as $\sigma_n$ increased below this ligament length range.

According to Eq. (5), when ligament length exceeds the minimum of either $W/3$ or $2R_p$, then either the edge effects become significant ($L > W/3$) or that crack propagation begins before ligament length is fully yielded ($L > 2R_p$). However, EWF studies have frequently shown, e.g. Refs. [1,6,13,15–19,21,22] that the proposed upper bound limit is too stringent as linearity between $w_f$ and $L$ is seen to extend well beyond the limit $W/3$. Results obtained here further corroborate this, as departure from linearity in $w_f$ versus $L$ plots seems to occurs at a ligament length value of about 16 and not 11.67 mm (= $W/3$). Mai [3] has stated that the departure from linearity in the upper region has no relation to the minimum of $W/3$ or $2R_p$, For the same reason an arbitrary maximum ligament length value of 15 mm is recommended by the ESIS protocol [11]. Although our results support Mai's view on $W/3$, at this stage we cannot confirm his view on $2R_p$, since

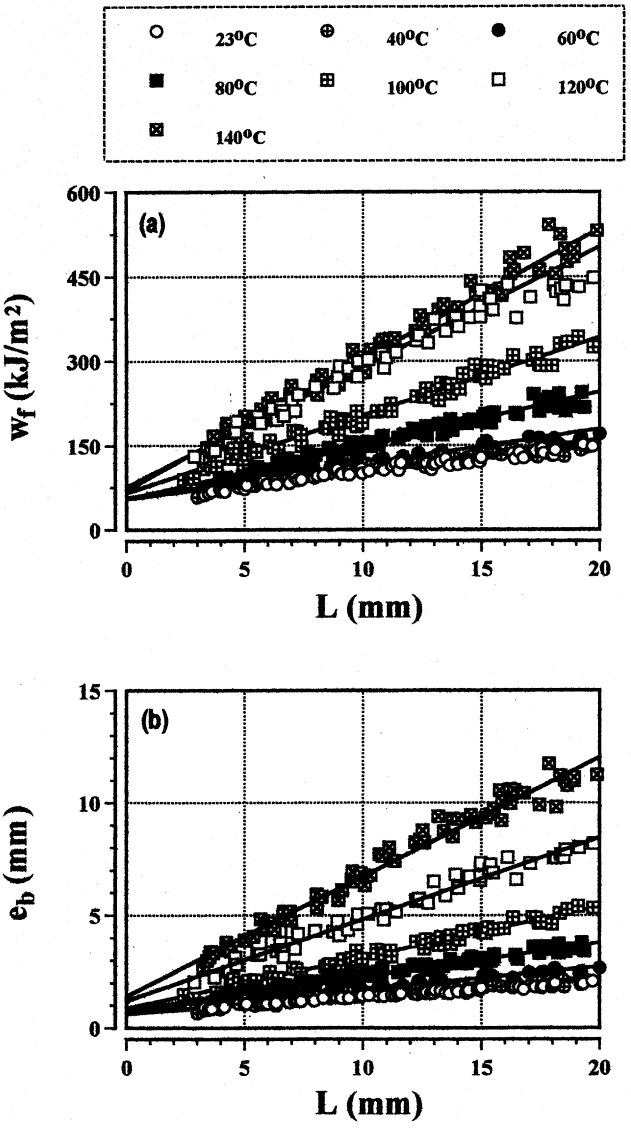


Fig. 9. Specific work of fracture ($w_f$) versus ligament length ($L$) as a function of temperature for all three thicknesses.

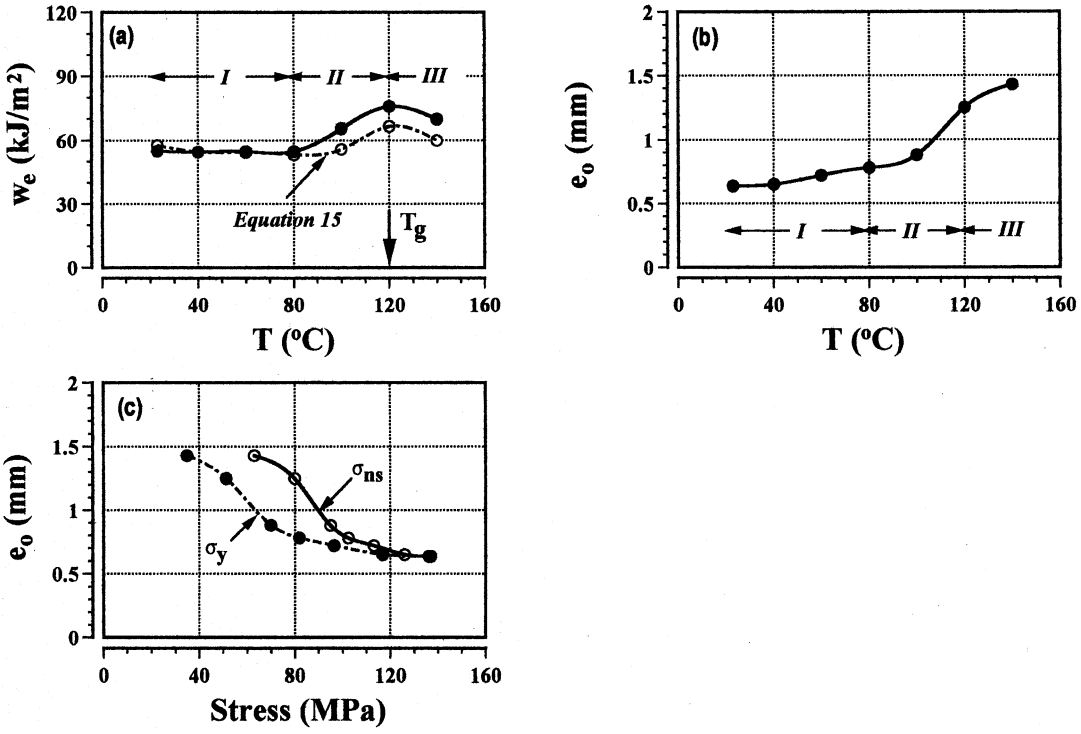


Fig. 10. Plots of: (a) specific EWF ($w_e$) versus temperature ($T$), (b) crack opening displacement ($e_0$) versus temperature ($T$), (c) crack opening displacement ($e_0$) versus stress ($\sigma_y$ and $\sigma_{ns}$).

according to Eq. (6), estimation of $2R_p$ is only possible once $w_e$ is determined.

*4.2.2. Effect of temperature, T*

Fig. 9a gives a clearer indication of the way in which test temperature influences the relationship between $w_f$ and $L$ for the DENT type specimens (note: data points for all three thicknesses are represented by one symbol only). It can be seen that $w_f$ and the slope of the line both increase with temperature; the later implies that $\beta w_p$ increases with ductility.

To obtain values of the specific essential ($w_e$) and non-essential ($\beta w_p$) work of fracture, the valid ligament length range was defined here as 5 mm $\leq L \leq$ 16 mm and the $w_f$ values within this ligament length range were then extrapolated linearly to $L = 0$, as suggested by Eq. (3). Since variation of $w_f$ with $L$ at any given temperature is not particularly sensitive to thickness (see Fig. 8), a single linear extrapolation was performed on all the data points belonging to one test temperature. The values of $w_e$ and $\beta w_p$ obtained in this way for the DENT type specimens are given in Table 1.

As shown in Fig. 10a, $w_e$ shows three regions of varying temperature dependence:

(i) *Region I* ($23°C \leq T \leq 80°C$) : $w_e$ is more or less independent of temperature, having an average value of 54.76 kJ/m$^2$ for DENT type specimens.
(ii) *Region II* ($80°C < T \leq T_g$) : $w_e$ increases with temperature and peaks near the glass transition temperature of the polymer ($T_g \approx 120$–$125°C$). The maximum value is 75.72 kJ/m$^2$.
(iii) *Region III* ($T > T_g$) : $w_e$ decreases with increasing temperature.

It has been shown that $w_e$ may be related to net-section stress ($\sigma_{ns}$) and the critical crack opening displacement ($\delta_c$) by the following equation, e.g. Refs. [4,9,13,16,20]

$$w_e = 0.67\sigma_{ns}\delta_c \tag{15}$$

Wu and co-workers used a similar equation to explain the temperature dependence of $w_e$ in PBT/PC/IM blend [3]. For example, they argued that since $\delta_c$ and $\sigma_y$ are temperature-dependent, then for $w_e$ to decrease with increasing temperature, the decrease in $\sigma_y$ should outweigh the increase in $\delta_c$ with temperature.

According to Eq. (15), to obtain the three regions of varying temperature dependence for $w_e$ in Fig. 10a, $\sigma_{ns}$ and $\delta_c$ must compete in each region as stated below:

- *Region I.* Decrease in $\sigma_y$ with temperature should compensate the increase in $\delta_c$.
- *Region II.* Increase in $\delta_c$ with temperature should outweigh the decrease in $\sigma_y$.
- *Region III.* Decrease in $\sigma_y$ with temperatures should outweigh the increase in $\delta_c$.

It has been shown that the relationship between extension to break, $e_b$, and the ligament length is similar to that of $w_f$

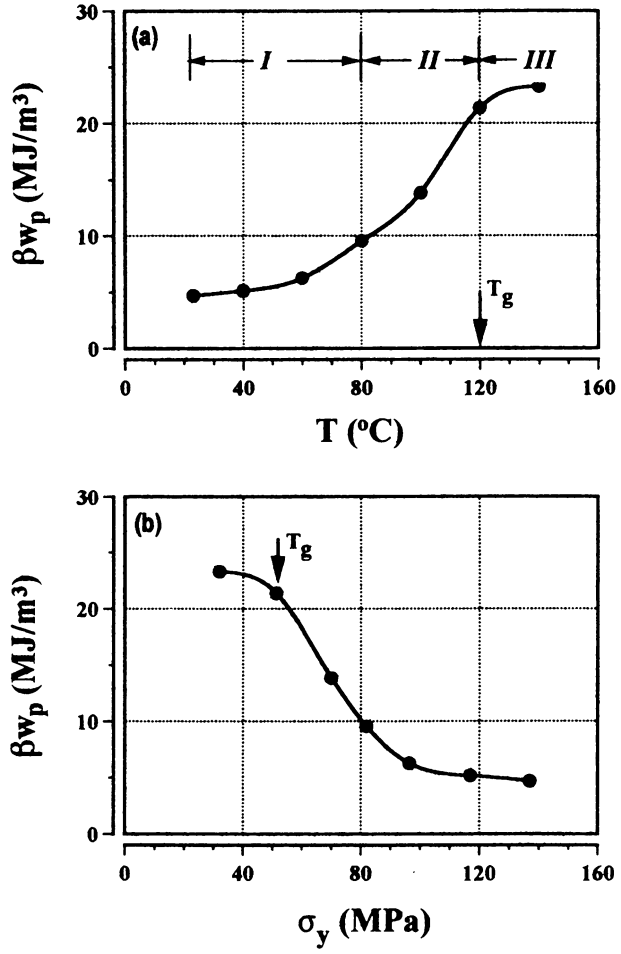


Fig. 11. Plots of: (a) specific non-essential work of fracture ($\beta w_p$) versus temperature ($T$), (b) specific non-essential work of fracture ($\beta w_p$) versus yield stress ($\sigma_y$).

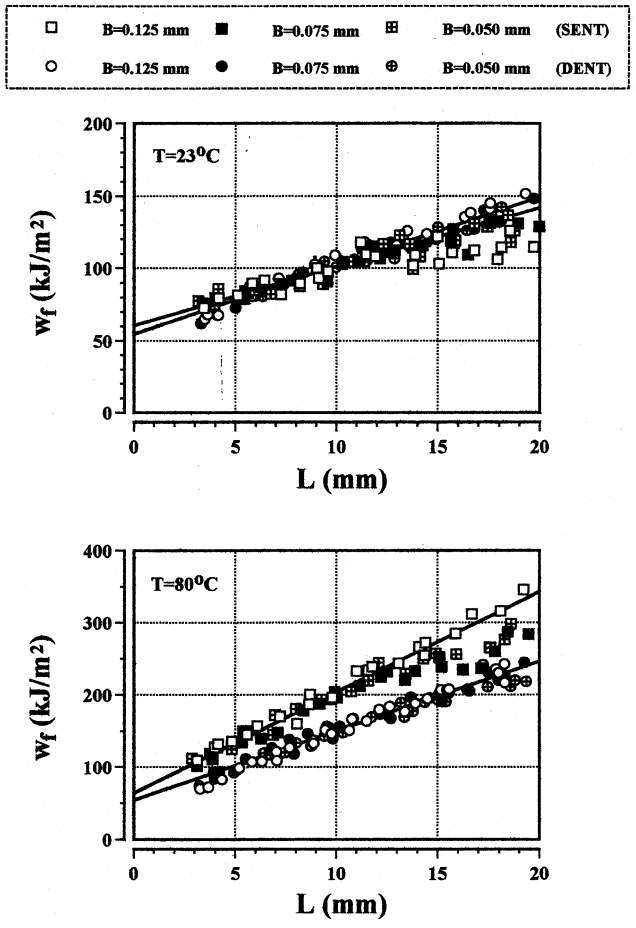


Fig. 12. Specific work of fracture ($w_f$) versus ligament length ($L$) for DENT and SENT type specimens for all three thicknesses at: (a) $T = 23$°C and (b) $T = 80$°C.

versus $L$ and thus may be expressed as, e.g. Refs. [1,4,9,13,16,20,22]:

$$e_b = e_0 + e_p L \tag{16}$$

where $e_0$ is the extrapolated value of $e_b$ at zero ligament length and $e_p$ is the plastic contribution to extension. The intercept value, $e_0$, has been identified as being equivalent to the critical crack opening displacement (COD), i.e. $e_0 \cong \delta_c$.

It can be deduced from Fig. 9b that variation of $e_b$ with ligament length is not affected by the thickness of the specimen, but increases with increasing temperature. To determine the dependence of $\delta_c$ on temperature, the plot in Fig. 9b were interpolated linearly to $L = 0$ as suggested by Eq. (16). The extrapolated values of $e_0$ are given in Table 1 and plotted against temperature in Fig. 10b where it can be seen that $e_0$ increases with temperature in all three regions. It is also evident from Fig. 10c that $e_0$ decreases with increasing yield stress ($\sigma_y$) and net-section stress ($\sigma_{ns}$) and that the rate of change of $e_0$ with either stress is different in the three temperature regions in question. The predicted values of $w_e$ based on Eq. (15) are shown in Fig. 10a where it can be seen, that they agree reasonably well with the directly measured values, both in magnitude and variation with temperature.

As regards $\beta w_p$, it can be seen from Fig. 11a that this parameter increases with increasing temperature in all three regions and decreases with increasing yield stress as shown in Fig. 11b. Evidently, while $\beta w_p$ rises with temperature relatively slow in regions I and III, it rises steeply with temperature in region II. Since $w_p$ generally decreases with increasing temperature, $\beta$ must therefore increase with temperature.

Finally, the size of the plastic zone ($2R_p$) was calculated at each temperature using Eq. (6). From the values listed in Table 1 it can be deduced that $2R_p < W/3$ for $T \leq 40$°C and $2R_p > W/3$ for $T \geq 60$°C. The departure from the linearity therefore bears no relation to the min($W/3$ or $2R_p$).

*4.2.3. Effect of specimen geometry*

The effect of specimen geometry on EWF was studied at 23 and 80°C only. Plots of $w_f$ versus $L$ for DENT and SENT type specimens at these two temperatures for all three thicknesses are compared in Fig. 12. Plots show variation for SENT type specimens is reasonably linear and like DENT

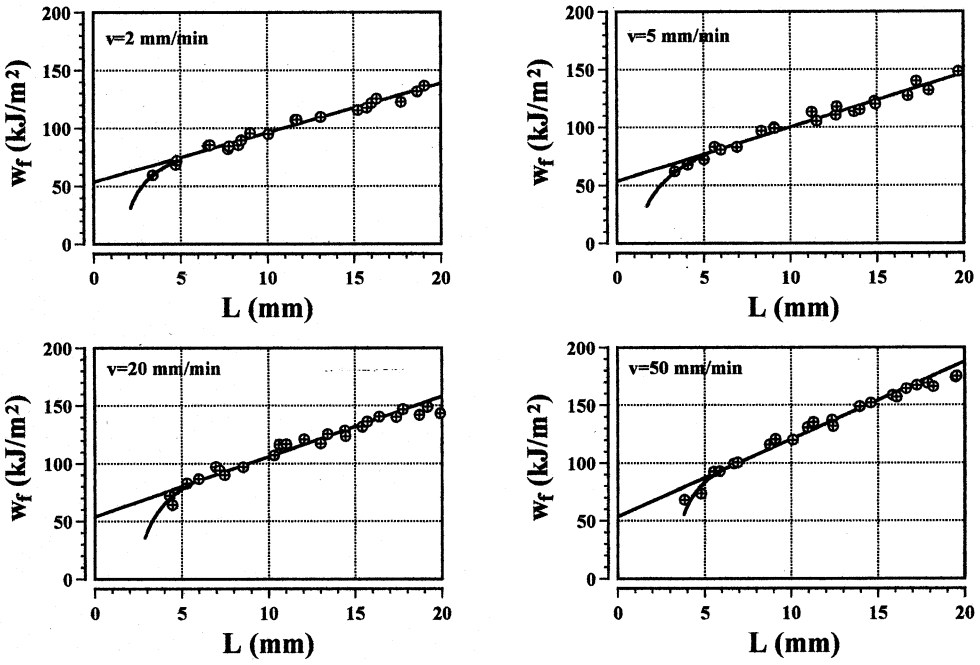


Fig. 13. Plots of specific work of fracture ($w_f$) versus ligament length ($L$) for DENT type specimens of thickness 0.075 mm as a function of loading rate.

type specimens is independent of thickness. However, the upper ligament length threshold value for SENT specimens appears to be 13 mm compared to 16 mm obtained for DENT specimens. Beyond this ligament length value, SENT data are very scattered. This is thought to be due to unstable failure of the SENT specimens after maximum load, at large ligament lengths.

Although $w_e$ values obtained via SENT specimens are higher than DENT specimens (see Table 1) they nevertheless confirm the temperature independence of $w_e$ in region I.

Finally, it can seen from Table 1, that $\beta w_p$ for SENT specimens like DENT specimens, increases with increasing temperature.

#### 4.2.4. Effect of deformation rate, v

Fig. 13 shows plots of $w_f$ versus $L$ for DENT type specimens of thickness 0.075 mm at loading rate values of 2, 5, 20 and 50 mm/min ($T = 23$°C). Plots show that good linearity is obtained for ligament lengths in the range 5 mm $\leq L \leq$ 16 mm. The specific essential work and non-essential work of fracture values are summarised in Table 2. It can be seen that $w_e$ is more or less independent of rate.

Table 2
Effect of loading rate on work of fracture parameters ($B = 0.075$ mm, $T = 23$°C)

| | Loading rate (mm/min) | | | |
|---|---|---|---|---|
| | 2 | 5 | 20 | 50 |
| $w_e$ (kJ/m$^2$) | 53.94 | 53.83 | 54.01 | 53.84 |
| $\beta w_p$ (MJ/m$^3$) | 4.24 | 4.65 | 5.21 | 6.69 |

This observation is consistent with previous findings by the authors [13,22] and other co-workers, e.g. Refs. [5,12,15–17] covering a wide range of polymers. As regards $\beta w_p$, it can be seen from Table 2 that this parameter increases with loading rate.

### 4.3. J-Integral

Fig. 14 shows $J_R$-curve for all the three thicknesses at 23 and 80°C. It can be see that the $J_R$ curve is independent of the thickness at both temperatures as indeed were the plots of $w_f$ versus $L$. The data points falling between exclusion lines 0.05 and 1.8 mm (10% of the original ligament length) were curve fitted according to Eq. (12) and the $J_{0.2}$ value at each temperature was then obtained according to Eq. (13). Additionally, the linear part of the $J_R$-curves were extrapolated linearly to $\Delta a = 0$ as suggested by Wu and Mai [6] to obtain $J_0$ (value of the $J$-integral at $\Delta a = 0$). It can be seen from Table 1 that difference between $J_{0.2}$ and $J_o$ is not significant and both agree quite well with $w_e$. It must be noted however, that although $J_{0.2}$ values satisfy the $J$-controlled growth requirement linked to the ligament length (i.e. $W - a$) they fail to satisfy the requirement linked to the specimen thickness, $B$ (see Table 1). It must be said that since these requirements are for determination of $J_{0.2}$ under plane-strain conditions, thus the $J_{0.2}$ values reported here are measured under plane-stress conditions.

Table 1 also compares values of $dJ/da$ with $\beta w_p$ where it can be seen that $dJ/da$ values are much greater than $\beta w_p$ values.

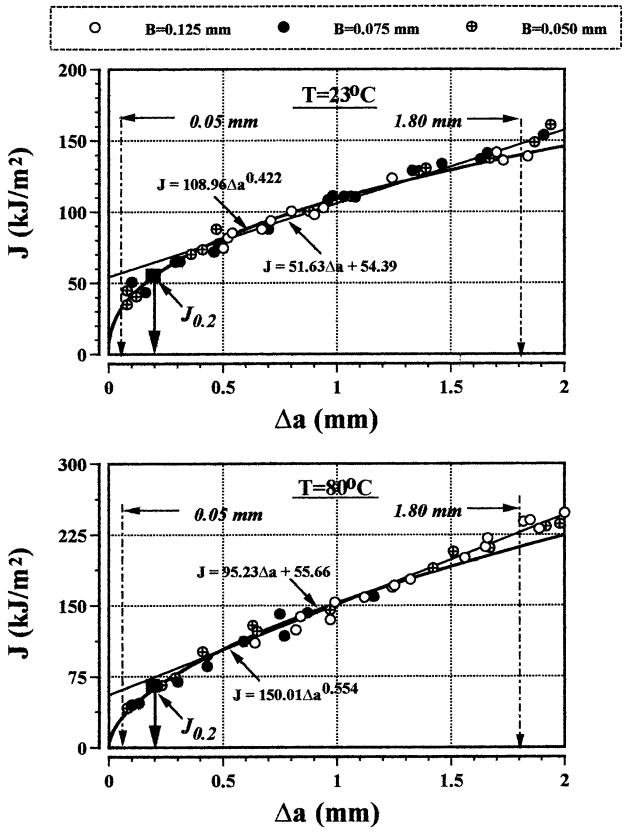


Fig. 14. Plots of $J$ versus crack extension ($\Delta a$) for SENT type specimens at: (a) $T = 23$°C and (b) $T = 80$°C.

## 5. Conclusions

Fracture toughness of a semi-crystalline PEN film was measured as a function of specimen thickness, specimen geometry, test temperature and the loading rate. Results indicated:

(i) $w_e$ and $\beta w_p$ are both independent of thickness but vary with test temperature.
(ii) $w_e$ showed three regions of varying temperature dependence; it was independent of temperature between 23 and 80°C (having average value of ≈54.76 kJ/m$^2$), increased with temperature between 80 and 120°C and reached a maximum value of 75.72 kJ/m$^2$ at glass transition temperature (i.e. 120°C) and decreased thereafter. On the other hand, $\beta w_p$ increased with temperature in all three regions. The greatest increase in $\beta w_p$ value occurred in region II.
(iii) $w_e$ was independent of loading rate but $\beta w_p$ increased with increasing rate.
(iv) SENT type specimens gave higher $w_e$ value compared to DENT specimens.
(v) $J_R$-curve was independent of thickness but was dependent on temperature. Values of $J_{0.2}$ and $J_0$ showed no significant variation with respect to temperature. $w_e$ was found to be equivalent to $J_{0.2}$ (or $J_0$).

## Acknowledgements

The authors are thankful to the Dupont UK for the provision of the material.

## References

[1] Mai YW, Cotterell B, Horlyck R, Vigna G. Polym Engng Sci 1987;27:804.
[2] Paton CA, Hashemi S. J Mater Sci 1992;27:2279.
[3] Wu J, Mai YW, Cotterell B. J Mater Sci 1993;28:3373.
[4] Hashemi S, Yuan Z. Plast Rubber Compos Process Appl 1994;21:151.
[5] Chan WYF, Williams JG. Polymer 1994;35:1666.
[6] Wu J, Mai YW. Polym Engng Sci 1996;36:2275.
[7] Levita G, Paris L, McLoughlin S. J Mater Sci 1996;31:1545.
[8] Karger-Kocsis J, Czigany T. Polymer 1996;37:2433.
[9] Hashemi S. J Mater Sci 1997;32:1573.
[10] Karger-Kocsis J, Czigany T, Moskala EJ. Polymer 1997;38:4587.
[11] Test protocol for essential work of fracture, Version 5, ESIS TC-4 Group, Les Diablerets, 1998.
[12] Karger-Kocsis J, Czigany T, Moskala EJ. Polymer 1998;39:3939.
[13] Arkhireyeva A, Hashemi S, O'Brien M. J Mater Sci 1999;34:5961.
[14] Ferrer-Balas D, Maspoch ML, Martinez AB, Santana OO. Polym Bull 1999;42:101.
[15] Ching ECY, Li RKY, Mai YW. Polym Engng Sci 2000;40:310.
[16] Hashemi S, Williams JG. Plast Rubber Compos 2000;29:294.
[17] Hashemi S. Polym Engng Sci 2000;40:132.
[18] Hashemi S. Polym Engng Sci 2000;40:798.
[19] Hashemi S. Polym Engng Sci 2000;40:1435.
[20] Mouzakis DE, Karger-Kocsis J, Moskala EJ. J Mater Sci Lett 2000;19:1615.
[21] Arkhireyeva A, Hashemi S. Plast Rubber Compos 2001:30.
[22] Arkhireyeva A, Hashemi S. Plast Rubber Compos, submitted for publication.
[23] Broberg KB. Int J Fract 1968;4:11.
[24] Sumpter JD, Turner CE. Int J Fract 1973;9:320.
[25] D 6068, Standard Test Method for Determining $J$–$R$ curves of Plastic Materials, American Society for Testing Materials, Philadelphia, 1996.
[26] ESIS Technical Committee on Polymers and Composites A Testing Protocol for Conducting $J$-Crack Growth Resistance Curve Tests on Plastics, May 1995.
[27] Hill RH. J Mech Phys Solids 1952;1:19.